EFFECTS OF ALUMINUM AND IRON NANOPARTICLE ADDITIVES ON COMPOSITE AP/HTPB SOLID PROPELLANT REGRESSION RATE

By

Jeremy A. Styborski

A Thesis Submitted to the Graduate Faculty of
Rensselaer Polytechnic Institute
In Partial Fulfillment of the Requirements for the Degree of

MASTER OF SCIENCE

Major Subject: Aeronautical Engineering

Approved by the
Examining Committee:

_____
Matthew Oehlschlaeger
Committee Chair and Thesis Advisor

_____
Kurt Anderson, Member

_____
Riccardo Bevilacqua, Member

Rensselaer Polytechnic Institute
Troy, New York

April 2014
(For Graduation May 2014)

CONTENTS

LIST OF TABLES

LIST OF FIGURES

NOMENCLATURE

AP	Ammonium Perchlorate
HTPB	Hydroxyl-Terminated Polybutadiene
PBAN	Polybutadiene Acrylonitrile
$\dot{m}$	Fuel Consumption Rate
ρ	Solid Propellant Density
A_s	Burning Surface Area
$\dot{r}$	Flame Regression Rate
a	Regression Rate Law Temperature Coefficient
P	Ambient Pressure
n	Regression Rate Pressure Exponent
GDF	Granular Diffusion Flame
BDP	Beckstead-Derr-Price
PEM	Petite-Ensemble Model
COR	Continuous Oxidizer Regression
RPI	Rensselaer Polytechnic Institute
SEM	Scanning Electron Microscope
PAPI	Polymethylene Polyphenylisocyanate
L	Strand Length
FR	Camera Frame Rate
F_{fo}	Flame-out Frame Number
F_{ign}	Ignition Frame Number

ACKNOWLEDGEMENTS

I would like to acknowledge the support given by my research professor and academic advisor, Dr. Matthew Oehlschlaeger. With his patience and encouragement, this experiment and experiment setup was conceived, constructed, and successfully used within my time here at Rensselaer Polytechnic Institute. My thesis committee, consisting of Professor Matthew Oehlschlaeger, Professor Kurt Anderson, and Professor Riccardo Bevilacqua, have all influenced me on my path to working in combustion and propulsion.

I would also like to recognize my friends and colleagues who have worked with me on this project. Specifically, I'd like to thank Matthew Scorza, Melissa Smith, Manuel Franco, Jeffrey Mockelman, Colin Lenhoff, and Wesley Rudy. Sandeep Gowdagiri, Mingdi Huang, Weijing Wang, Aniket Tekawade, and Will Gerken have all readily offered advice and assistance throughout the project. Not only was I able to complete a successful experiment with their help, but they made my stay at the Combustion and Energy Systems Laboratory an enjoyable and memorable experience.

Finally, I'd like to thank my family for their continual support throughout my life and my academic career. Without them and their soft guidance, I wouldn't have been able to become the individual I am today, nor accomplish what I have.

ABSTRACT

This project was started in the interest of supplementing existing data on additives to composite solid propellants. The study on the addition of iron and aluminum nanoparticles to composite AP/HTPB propellants was conducted at the Combustion and Energy Systems Laboratory at RPI in the new strand-burner experiment setup. For this study, a large literature review was conducted on history of solid propellant combustion modeling and the empirical results of tests on binders, plasticizers, AP particle size, and additives.

The study focused on the addition of nano-scale aluminum and iron in small concentrations to AP/HTPB solid propellants with an average AP particle size of 200 microns. Replacing 1% of the propellant's AP with 40-60 nm aluminum particles produced no change in combustive behavior. The addition of 1% 60-80 nm iron particles produced a significant increase in burn rate, although the increase was lesser at higher pressures. These results are summarized in Table 2. The increase in the burn rate at all pressures due to the addition of iron nanoparticles warranted further study on the effect of concentration of iron. Tests conducted at 10 atm showed that the mean regression rate varied with iron concentration, peaking at 1% and 3%. Regardless of the iron concentration, the regression rate was higher than the baseline AP/HTPB propellants. These results are summarized in Table 3.

1. INTRODUCTION

Solid combustibles have a wide range of uses, from applications in demolition, to deploying airbags in cars, to forcefully separating stages in space-vehicles, to fueling pulse detonation engines. However, the typical use of solid combustibles is as propellant for missiles, ICBMs, and rockets. Solid propellants are often favored because of their long storage lives, relatively low manufacturing costs, high thrust, and simple designs. Composite solid propellants, comprised of a powdered oxidizer within a rubber binder matrix and solidified with a curative, have high specific impulses relative to other solid propellants and tend to be more stable. Ammonium perchlorate (AP) is a typical oxidizing agent used in composite solid propellants due to its higher performance relative to ammonium nitrate. Many propellant formulations will use a bimodal distribution of oxidizing powders since AP particle size is linked to the burning rate of AP/HTPB composite propellant (Kohga, 2008). Typical liquid rubber fuels are hydroxyl-terminated polybutadiene (HTPB) and polybutadiene acrylonitrile (PBAN). A curative is added in a small percentage to solidify the rubber binder. Finally, high energy-density fuels, such as aluminum, can be added to the mixture in addition to the rubber fuel.

Both the thrust and specific impulse of a propellant combination are tightly linked to the mass flow rate of the propellant. The mass flow rate can be written as a function of the linear regression rate of the propellant surface over a given surface area, as shown in Equation 1.

$$\dot{m} = \rho A_s \dot{r} \tag{1}$$

The regression rate is usually determined experimentally, and has been shown to have power-law dependence on the combustion chamber pressure for a majority of solid propellants. Equation 2 shows the relation between regression rate and ambient chamber pressure, known as the regression rate law.

$$\dot{r} = aP^n \tag{2}$$

The constant coefficient, a, is the temperature coefficient. The pressure exponent, n, determines burn rate stability. For $n<1$, stable combustion occurs since any pressure increases would not lead to exponential acceleration of the regression rate.

Solid propellants typically follow Equation 2 closely. However, some propellants display plateau burning rate in which the burning rate tends to increase and then plateau as pressure increases. This 'anomalous' burning was noted by Summerfield et al. (1968) to occur for propellants with a relatively low percentage of solid propellants and is the subject of a paper by Stephens et al. (2009).

The primary drawback of solid rocket propellants is the lack of control over the fuel consumption rate. Once the propellant is ignited, it burns continuously at a rate determined Equation 2 until depleted. In order to influence the regression rate and burn time of a propellant, multiple methods are used. Perhaps the simplest way is to change the shape of the propellant grain to change the burn surface area. The subject of solid propellant grain design has garnered interest and many designs have been proposed and analyzed (Stone, 1958). However, the investigation into tailoring the solid propellant formulation itself has attracted even more attention and creates one of the largest areas of research in the rocket propulsion industry. Small changes in propellant chemistry have the ability to significantly affect the combustion behavior, especially when operating over large pressure and temperature ranges. The tailoring of the composite formula allows engine designers to control the thrust and burn rate of the engine by choosing between various mixes or layering them so that different burn characteristics appear as fuel is consumed. AP propellants have been shown to be particularly susceptible to regression rate tailoring (Parr, 1998). Apart from simply altering the proportions of the ingredients of a composite propellant, small percentages of additives may act as mixture catalysts in the condensed phase, reaction catalysts in the gas phase, additional ignition sources, or heat feedback systems. Additives are typically metal oxides and aluminum nanoparticles that comprise roughly 1% of the composite propellant (Sutton, 2008).

The addition of nanoscale particles to a composite propellant formulation provides advantages over the use of larger additives. The first is the increase in surface area-to-volume ratio due to the small particle size. Fujimura and Miyake show that the thermal decomposition rate of AP varies inversely with the specific surface area of a TiO_2

additive (Fujimura, 2010). Another possible advantage is the more exact control exercised during the synthesis of nanoparticles. The ability to process nanomaterials from scratch allows precise control over the chemical components, surface chemistry, and molecular structure (Chen, 2006).

The motive for this research was the existence of a multitude of research into the addition of nanoscale metal oxides to composite solid propellants and the relatively small number of studies into the addition of nanoscale metals, specifically iron. This study investigates the effects of iron nanonparticle concentration and ambient pressure on the regression rate of composite AP/HTPB propellants. Experimental data on the effect of ambient pressure on aluminum nanoparticle-laced AP/HTPB propellant is also presented in order to compare with previous works. The literature review section provides an examination of models, experimental results, and theories regarding the addition of nanoparticle additives to solid propellants. The experimental procedure section describes the mixing and testing procedures employed and assesses the uncertainties involved. Finally, experimental results are presented and possible explanations are discussed in the results section of the report.

2. BACKGROUND

In order to understand the mechanisms of solid propellant combustion and the effects of formulation tailoring, a comprehensive literature survey was performed. The highlights are provided below. First, the past and current models used for characterizing composite AP/HTPB combustion behavior are explained and analyzed. Once the overarching models for AP/HTPB composite solid propellants are understood, the effects of formulation modification can be more thoroughly examined through experimental results. The effects of AP particle size and distribution are analyzed. Then, the role of HTPB and curative in the propellant is examined. Finally, the experimental trends and models for the effects of additives to AP/HTPB are reviewed.

2.1 Composite Solid Propellant Combustion Modeling

The first model that accurately represented the combustion of most types of AP composite propellants was devised by researchers at Princeton in the late 1950's and 1960's. The Granular Diffusion Flame (GDF) model is a relatively simple model in which a steady, one-dimensional flame near the propellant surface propagates uniformly into the propellant. Finite-sized fuel and oxidizer pockets are released through sublimation and pyrolysis. The pockets mix and react exothermically within the diffusion flame to form combustion products. Heat from the flame and combustion products is transferred via conduction alone to continue the release of the fuel and oxidizer pockets. The authors proposed a regression rate formula similar to the commonly used one. The equation agreed well with experiments conducted for AP composite propellants with high AP content, medium sized AP particles (~100μm), and ambient pressures of 1-100atm (Summerfield, 1969).

The Hermance model was developed in the mid-1960's as a more descriptive alternative to the GDF model. The primary concept of the Hermance model is the process by which oxidizer crystals decompose to react with pyrolyzed fuel-binder products in fissures between the oxidizer crystals and binder matrix. The final fuel and oxidizer decomposition products react in a diffusion flame above the surface of the propellant. In this new model, the processes that govern the one-dimensional flames regression into the

propellant are allowed to vary with temperature and pressure. The proposed formulas for regression rate and flame and surface temperatures are solved iteratively. The Hermance model maintained excellent agreement with experiments with pressures between 1-400atm and a range of average AP particle sizes. The model succeeded in accounting for distributed oxidizer particle size using a statistical average and for the increase in the regression rate pressure exponent, both areas in which the GDF model faltered (Hermance, 1966). However, the simple existence of the fissures that were crucial to the Hermance model was contested by the authors of the next model proposed for composite AP solid propellants.

In 1970, Beckstead, Derr, and Price published a paper proposing an eponymously-named model that considered multiple flames and paid special attention to the balance between diffusion and premixed flames as a function of pressure and AP particle size. The Beckstead, Derr, and Price (BDP) model assumed that a diffusion flame encompassed the circumference of AP particles entrenched in the binder matrix. This "primary flame" would exist at all pressures near the edges of the oxidizer crystals where the gasified fuel and AP products had time to mix. For small AP particle diameters and low ambient pressures, this flame dominates as the fuel and oxidizer particles have time to mix. For higher pressures or larger AP particle sizes, the primary flame recesses to the edges of the oxidizer crystals and an AP decomposition flame forms directly above the AP crystal due to the slower diffusion rate. Diffusion between AP monopropellant flame products and residual fuel products occurs and a secondary diffusion flame forms above the AP monopropellant flame. Like Hermance's model, the BDP model assumes a statistically average particle size. The BDP model requires an iterative process to determine burning rate and surface temperature. From experiments with unimodal, polysulfide composite propellants, the BDP model was shown to predict the dependence of burning rate on oxidizer concentration well, especially for propellants with average oxidizer particle sizes near 20 microns. Finally, the model tended to overestimate the effect of oxidizer particle size (Beckstead, 1970).

Like Hermance's model, the BDP model only considers the statistically-average oxidizer particle around which reactions occurred. Robert Glick pointed out this led to errors in the continuity equation because the oxidizer mass flux is dependent on the

oxidizer surface area. He proposed a correction that accounts for a range of oxidizer particle sizes (Glick, 1974). The Petite-Ensemble Model (PEM) was the first to incorporate this correction. It assumes a propellant flame structure identical to that of the BDP model and requires the satisfaction of the same energy relations. However, the PEM considers the regression rate for each of a range of oxidizer particle sizes and then computes an average regression rate. The PEM does assume some averaged parameters, such as oxidizer crystal height above the binder matrix and surface geometry. The PEM is solved in a manner similar to the BDP model (Renie, 1982).

Many models developed after the PEM contained characteristics and combustion mechanisms similar to or based off of the models mentioned above. In fact, the BDP model is the basis for the primary physical models used in the field of AP solid propellants today. Therefore, an adequate understanding of the theorized combustion mechanisms for composite solid propellants is achieved through understanding the above models. However, others have proposed additional models which account for other observed phenomena. In 1979, M.K. King proposed a model that accounted for subsurface reactions between fuel and oxidizer as well as changing oxidizer height as the fuel combusts. This model also allows different burning rates between fuel and oxidizer components. King later developed a model for erosive crossflow burning that would be heavily sourced in the development of rocket engines (1981). The Continuous Oxidizer Regression (COR) model follows the PEM but discards the assumption of an averaged oxidizer/binder surface geometry, instead calculating the instantaneous burning rate for a changing surface geometry (Cor, 1986). Hegab et al. (2001) created a combustion model based on the BDP model but ignored the primary diffusion flame, claiming that its effect is negligible. This 2 step chemical kinetics model was similar to multiple other models of the time. Citing poor predictions of the effects of AP fraction variations in 2 step models, Massa, Jackson, and Buckmaster (2005) added a third step to the chemical kinetics model. This 3 step model accounted for the primary diffusion flame in which non-decomposed AP products react with pyrolyzed HTPB products. The authors claimed better agreement with experiment and Miller Pack simulation compared to the previous 2 step models. Ramakrishna, Paul and Mukunda (2002) had previously produced a similar 3 step chemical kinetics model for sandwich propellants based off of 2-dimensional

unsteady Navier-Stokes equations. Cai, Thakre, and Yang (2008) provide a concise description of past models as well as a numerical model of the processes governing the combustion of AP/HTPB propellants based on a flame structure similar to that proposed by the BDP model. The model employs the conservation equations to model gas-phase diffusion processes and a one-step reaction model to account for chemical kinetics between AP and HTPB. AP decomposition is considered separately. Gross and Beckstead (2011) produced simulated results from a numerical model detailed in their previous works (Gross, 2009). The model showed good agreement with experimental data. The model asserts that a single AP composite propellant flame, composed of an AP monopropellant flame, a homogenized binder (fine AP and HTPB) flame, and a primary diffusion flame, is held near the surface of the propellant, centered about coarse AP particles. A final diffusion flame is held above the AP composite propellant flame. The model predicts that the AP composite flame behaves similar to the primary flame of the BDP model.

2.2 Empirical Results for Composite Solid Propellants

While the above models were often supported by experimental data, there is a plethora of studies on AP/HTPB composite solid propellants that are purely experimental. The majority of the studies deal with the effects of average AP size, AP loading, AP particle size distribution, binder type, and the addition of conductive fibers or catalytic nanoparticles. The latter appears to be the most prolific. Very few studies on the effects of binder and hardeners appear to have been performed. The following paragraphs discuss the studies relating to experimental AP, binder, and additive studies.

Collins (1947) produced a thesis in which he studied the composite solid propellants in a closed bomb. Thiokol LP-3 fuel was paired with either AP, potassium perchlorate, or both. He found that the burn rate for the potassium perchlorate propellants was highest while the burn rate was lowest for the AP propellants. Parr and Hanson-Parr (1996) were able to observe the low diffusion flame standoff distances in AP propellants and therefore, help validate modern models of AP composite solid propellants. They claimed that the reactive AP decomposition products from the monopropellant flame accelerated the chemical kinetics within the diffusion zone to hold the diffusion flame

relatively close to the surface. Kohga (2008) parametrically studied the effects of AP particle size and distributions and coarse AP loadings in AP/HTPB propellants. He showed that, for identical ambient pressures, the burning rate was inversely related to AP particle size and directly related to AP loading. Bimodal propellants with higher coarse AP loadings also had lower burning rates. However, unimodal AP propellants tended to have higher burning rates compared to bimodal AP propellants with the same average particle size. Renie et al. (1979) explored the effects of AP distribution through the use of the PEM. They showed that average AP particle size was inversely correlated with burn rate. The model also predicted lower burning rates for bimodal propellants with higher ratios of coarse to fine AP, which is qualitatively in agreement with the results by Kohga. The authors showed that the model could predict burning rate and the pressure exponent to within 10% of its experimental value.

Cohen, Fleming, and Derr (1974) reported on the behaviors of various binders in composite solid propellants using AP. They show that the binders tend to melt and then boil or decompose at the propellant surface. The pyrolysis mechanisms for each binder tested were different but appeared to be independent of the presence AP or additives. The authors speculated that the interactions between the binder and AP were particularly important in the gas phase rather than at the burning surface. Jayaraman et al. (2009) showed that increases in plasticizer content led to lower plateau burning pressures.

Pearson (1971) reviewed the methods by which catalysts could affect the burning rate of solid propellants and provided possible chemical reaction mechanisms, specifically for AP decomposition. The number of possible methods by which catalysts could enhance burn rates was limited to four: the catalytic additive could accelerate fuel decomposition, accelerate perchloric acid decomposition, accelerate fuel/oxidizer reactions on the fuel surface, or accelerate gaseous reactions between AP decomposition products and fuel. The exact sites where these catalytic activities take place were not specified.

Solymosi et al. (1970) were able to classify catalysts for perchloric acid decomposition between ineffective and highly effective. They found that ferric and aluminum oxides, two of the most commonly studied additives, were among the most effective catalysts. Chromic, cupric, and nickel oxides were also highly effective.

Titanium oxide, which has also been highly studied, was classified as less active. Rastogi, Singh, and Singh (1977) studied the combustion of AP/Polystyrene composite solid propellants using ammonium dichromate and multiple carbonates and oxides of chromium and copper. They found that catalyzed propellants allowed increases in burning rate, flame temperature and decomposition rate for the oxidizers used. These increases were attributed to accelerated gas phase reactions rather than condensed phase reactions. Ammonium dichromate and carbonate additives were shown to be more effective than the oxides.

Strahle et al. (1974) studied the effects of copper chromite and ferric oxide to AP/HTPB composite sandwiches for pressures between 600-3200psia. Additives were tested in both the binder, the oxidizer and at the interface. The burn rate was enhanced most when the additives were added to the oxidizer and least when the additives were added at the interface. Copper chromite outperformed ferric oxide throughout the pressure range, peaking at a pressure of 2800 psia at about four times the burn rate of pure AP/HTPB. For both additives, it was concluded that there is no change in the binder pyrolysis processes. Rather, the additives catalyzed the AP processes and gas phase interactions. This result was similar to the results found by Cohen et al. (1974) using catalytic additives of n-butylferrocene and polycarbonanesiloxane in HTPB. Handley and Strahle also produced a subsequent paper (1975) that investigated additional additives in AP/HTPB composite sandwiches. They found that iron blue and ferrocene, when added to the oxidizer, enhanced the burn rate as much as ferric oxide at lower pressures (<1000psia) and less than ferric oxide at higher pressures (>1000psia). Copper chromite outperformed all three other additives at all pressures. Like the results of their previous paper, Handley and Strahle showed that the burn rate was barely influenced when the additives were placed in the binder. Chakravarthy et al. (1997) similarly added ferric oxide to the binder in oxidizer/binder sandwiches. They noted that the additive tended to concentrate at the burning surface and that the surface reactions and heat release are accelerated at contact lines between the binder and oxidizer. AP was specifically noted as a candidate for catalyzed gas phase reactions due to the release of reactive perchloric acid from decomposition. The presence of additives in the binder noticeably increased the burn rates of the sandwich propellants, unlike the other experiments mentioned above.

Stephens et al. (2009) provide an experimental study on the behavior of AP/HTPB propellants with titanium dioxide (titania) additives. This study focused largely on varying the crystal structure of the titania and on titania doping with aluminum, iron and gadolinium. A major focus of the paper was the correction of the plateau in burning rate as a function of pressure and mending it. The results showed that the additive allowed a relatively minor increase in burn rate, regardless of the crystal structure. Additions of titania was able to correct anomalous burning rate behaviors at higher AP loadings. This was attributed to viscosity changes in the binder melt layer at the burning surface of the propellant. Iron and gadolinium doped titania allowed the greatest increase in burn rate above the baseline out of the three doping types. The exact mechanism by which titania enhances burn rate isn't specified. The same group was responsible for another paper in 2010 that studied the addition of titania and cerium dioxide (ceria) to AP/HTPB composite solid propellants. None of the anomalous burning of the previous study was observed. The addition of additives increased the burn rate, titania being the more effective additive. However, the exact correlations are difficult to discern because of the multi-parameter nature of the study. Kreitz (2010) produced a thesis on the addition of titania to unimodal and bimodal AP/HTPB composite solid propellants. For unimodal propellants, 200 micron AP was used. For bimodal propellants, 23 micron AP was used in a 30:70 mass ratio with 200 micron AP. For all cases, the addition of 1% titania increased the burn rate of the propellant compared to the baseline. Average burn rate increases were higher for catalyzed unimodal propellants compared to the catalyzed bimodal propellants (with respect to their respective baseline propellants). Higher loadings of AP overall led to larger average burn rate increases. It's uncertain if this effect is due simply to the higher loading of AP or because of greater catalytic action associated with higher AP. Kreitz also showed that titania doped with either iron or aluminum produced higher burn rates compared to a unimodal baseline for various doping methods.

Yaman et al. (2014) produced a paper that concisely details the factors affecting the burn rate of solid propellants. They supplemented their review an experimental study on the effects of aluminum particle addition to a nitroglycerin/nitrocellulose double base propellant. They found that a higher loading of aluminum led to both higher burning

heats and higher burning rates (averaged over a range of pressures). Galfetti et al. (2007) analyzed the effects of micro- and nano-aluminum particles added to AP/HTPB composite solid propellants. Other binders were tested as well. The results showed that the increase in surface area and heat feedback offered by smaller catalysts led to increased reactivity and increased burning rate. Aluminum agglomeration was also decreased for smaller particle sizes. Sambamurthi et al. (1984) showed that the amount of aluminum agglomeration and the agglomerate sizes in AP based propellants was dependent on the aluminum particle size, pressure, and fine AP content (for bimodal propellants). The authors proposed simple scenarios by which the above factors interact to establish or extinguish individual AP particle flamelets, leading to the ignition or agglomeration of aluminum. Jayaraman et al. (2009) analyzed aluminum, titanium dioxide, and ferric oxide added to AP/HTPB composite solid propellants between 1-12MPa. The group also considered bimodal additions of micro- and nano-aluminum. The use of nano-aluminum in place of micro-aluminum increased burn rates by roughly 100%. However, the additional increases in burn rate due to the addition of titanium dioxide or ferric oxide catalysts are proportionally smaller for nano-aluminum. This effect is heavily dependent on the catalyst size, with micro-scale catalysts producing no additional effect for nano-aluminum propellant. Finally, the burning rate is inversely related to the coarse to fine ratio of aluminum added in bimodal additive propellants. The group demonstrates that increased burn rate with aluminum-doped propellants is associated with the heat feedback and ignition of aluminum accumulating at the surface of the propellant. Like the previous article, Jayaraman et al. proposed multiple scenarios in which aluminum accumulation, AP size and pressure could influence the burning rate. Liu et al. (2004) was also able to show that the presence of nano-metal powders decreased the decomposition temperature of AP.

3. EXPERIMENT AND PROCEDURES

Regression rate experiments were carried out for AP/HTPB/additive propellants in a strand burner apparatus developed as part of this thesis work. The entire process of propellant mixing and strand burning was conducted at the Combustion and Energy Systems Laboratory at Rensselaer Polytechnic Institute (RPI). This ensured that the quality desired in the propellants and testing was within control throughout the process. The following sections detail the steps required for mixing and curing the solid propellant, the experimental procedure, and the uncertainties associated with the experiment.

3.1 Propellant Composition

AP is a typical oxidizer used in the formulation of solid propellant rocket motors. The current work uses AP powder with an average particle diameter of 200 microns. An average particle size of 200 microns was chosen due to its use in multiple other studies. The powder is purchased from the Rolling Thunder Pyrotechnics Corporation. Figure 1 shows field emission scanning electron microscope (FESEM) images of the AP unground and ground (using the processes detailed in the mixing procedure section) AP particles. R45M HTPB is mixed with the AP powder in a ratio of roughly 1:4 by mass (the exact ratio depends on the amount of additive) and serves as the mixture binder and primary fuel. A polymethylene polyphenylisocyanate plasticizer (PAPI-94) is used as the mixture curative. The HTPB and PAPI-94 were procured as a single kit by Aerocon Systems. The binder-to-curative mixture ratio used is 7.33:1 by mass and is obtained from the distributor.

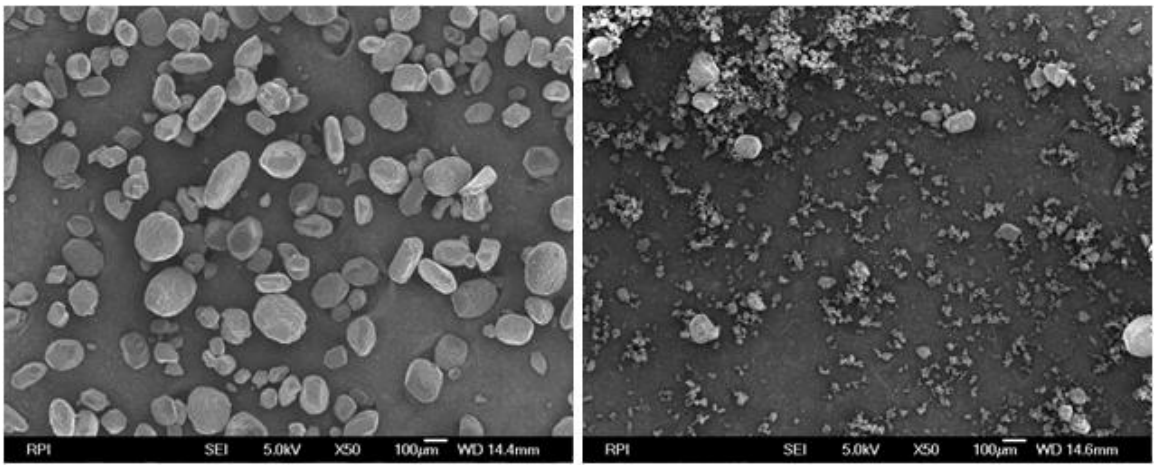

Figure 1: FESEM Images of Unground AP (left) and Ground AP (right) at 50X Magnification

Additives can be used in solid propellants in small percentages to enhance their burn rates. The current study investigates the effects of nano-scale iron and aluminum particles on the solid propellant regression rate. The aluminum nanoparticles have an average particle size between 40-60nm. The iron nanoparticles range between 60-80nm on average. Both additives are purchased from SkySpring Nanomaterials and maintain a purity of 99.9%. Figure 2 shows magnified images of the aluminum and iron nanoparticles, courtesy of SkySprings Nanomaterials Figure 2 shows FESEM images of the aluminum and iron nanoparticles used as additives.

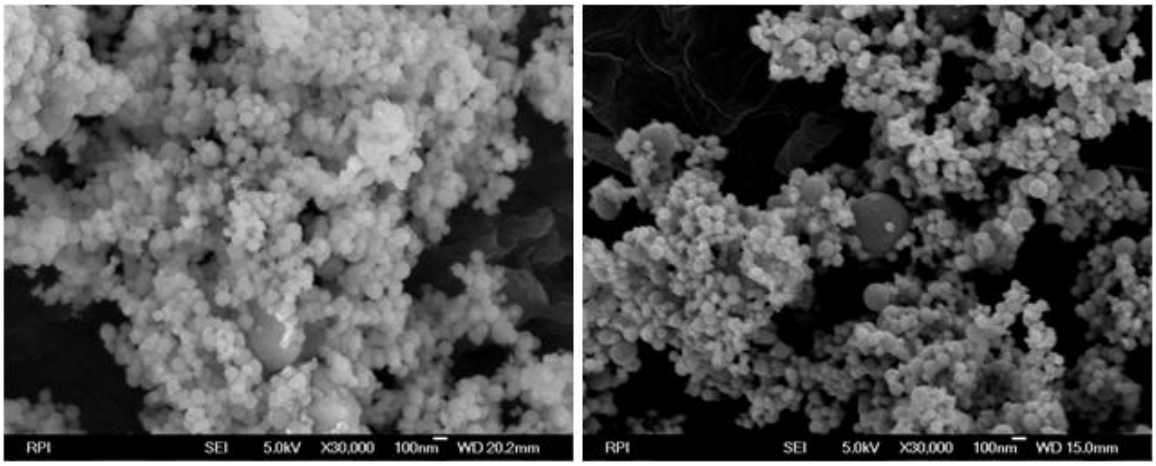

Figure 2: FESEM Images of Aluminum (left) and Iron (right) Nanoparticles at 30,000X Magnification

Propellant formulation can affect combustion characteristics of the solid propellant strands. Therefore, it's important to maintain a consistent method of formulation throughout all tests. The current study uses strands with a constant mass ratio between the dry and wet portions, following a precedent set by Jayaraman et al. (2009). All solid propellant mixes maintain a dry-to-wet mass ratio of 80.2:19.8. Thus, the combined masses of AP and additive comprises 80.2% of the solid propellant's mass while the combined masses of HTPB and PAPI-94 make up the remaining 19.8%. If any additives are added to the mix, they replace an equivalent mass of AP, maintaining a constant wet portion of the composite propellant. For example, strands of 3% iron additive would contain 3% iron and 77.2% AP by mass whereas control tests (with no additives) simply contain 80.2% AP by mass. Table 1 summarizes the permutations of propellant compositions used in this experiment. For regression rate versus pressure tests, only the control and 1% additive formulations were used (formulations A and C) over a pressure range of 1-100atm. For regression rate versus additive percentage tests, all formulations shown were tested with iron additive at an ambient pressure of 10 atm.

Table 1: Propellant Composition Percentage by Mass

	Dry		Wet			
Designation	**AP**	**Additive**	**HTPB**	**PAPI-94**	**Dry Total**	**Wet Total**
A	80.2	0	17.424	2.376	80.2	19.8
B	79.7	0.5	17.424	2.376	80.2	19.8
C	79.2	1	17.424	2.376	80.2	19.8
D	78.95	1.25	17.424	2.376	80.2	19.8
E	78.7	1.5	17.424	2.376	80.2	19.8
F	78.2	2	17.424	2.376	80.2	19.8
G	77.2	3	17.424	2.376	80.2	19.8

3.2 Propellant Mixing Procedure

Since all solid propellant mixes were comprised of AP, HTPB, the curative PAPI-94, and a trace additive, the mixing procedure for all strands studied was consistent. The strands were prepared using a hand-mixing technique that, by visual inspection, appears to uniformly distribute additives and eliminate gas pockets. The hand-mixing method used is adapted from the method employed by Texas A&M University (Kreitz, 2010).

The mixing procedure begins by massing of the components of the solid propellant mix. A Mettler AT200 scale with precision to 0.0001g is used to determine masses. Both dry components of the solid propellant mix are massed in separate stainless steel bowls and then combined in a mortar. The dry mix is then ground for 3-5 minutes using a pestle until the mixture appears to be homogenous and clumps have disappeared. The dry mix is then poured into a third, clean, stainless steel bowl. HTPB is suctioned into a syringe directly from its container so that its mass can be determined. Once the desired HTPB mass is achieved within the syringe, the binder is extruded into the dry mix of AP and additive. The resulting powder-binder mixture is hand-stirred with a Teflon mixing rod for roughly 5 minutes until a uniform paste is formed. Special care is taken to ensure that no dry mix or binder is left on the stirring rod or mixing bowl. In preliminary tests of the mixing procedure, the mixture of AP/HTPB/Additive was inserted into a vacuum chamber that lowered ambient pressure to 0.1 psia for roughly 15 minutes. The intent was to remove any gas pockets present within the mix. However, no visible changes in the consistency of the mixture were noticed. Concerns over contamination due to the particulate matter present in the vacuum lines caused this portion of the mixing procedure to be cancelled. All results shown in this paper are for strands created without the aid of a vacuum. After a satisfactory mix of HTPB, AP and additive is achieved, the curative, PAPI-94, is drawn and massed in a manner similar to that used to add HTPB, albeit with a pipette instead of a syringe. PAPI-94 is added to the paste-like mixture and hand-mixed with a Teflon mixing rod for roughly 5 minutes until the curative has been distributed thoroughly. This final mixture is then hand-kneaded to ensure a uniform mix. Sterile latex gloves are worn to avoid contamination.

After a successful mixture has been created, clear-white Teflon tubing with an inner diameter of 0.79 cm is cut into six 3.18 cm long segments. The propellant mixture is packed into the Teflon tubes and compacted using Teflon mixing rods. The choice to use Teflon tubes was inspired by its historical use (Carro, 2001). Pieces of the propellant mix are added to the tube in small amounts with compaction between each addition to ensure that no air pockets are formed. The clear-white tubing allows visual inspection of the propellant inside the tube. Sterile latex gloves are worn throughout the packing process. After the strands are packed by hand, they are loaded into a centrifuge for further

compaction. The centrifuge runs at roughly 500 rpm for 18 hours in air at room conditions, allowing the propellant to cure and compact simultaneously. The use of a centrifuge produces no noticeable separation of materials and the strands appear uniform along their axis after curing in the centrifuge.

In order to avoid any combustion anomalies due to surface phenomena (e.g., oxidation) as well as ensure consistent strand lengths, the 3.18 cm strand is cut down to 2.54 cm using a jig that secures the strand. A cleaned band-saw is guided through two slats in the jig to cut the strand perpendicular to its axis. The two slats are spaced 2.54 cm apart, with the strand sitting across them. The result is that both original ends of the strand are trimmed off and propellant that was unexposed to air during the curing process is exposed now that the propellant has cured. Figure 3 shows 1% iron additive strands that are the final products the mixing procedure above. The trimmed surface is easily viewed on the strand on the left. The propellant appears uniform throughout the strands.

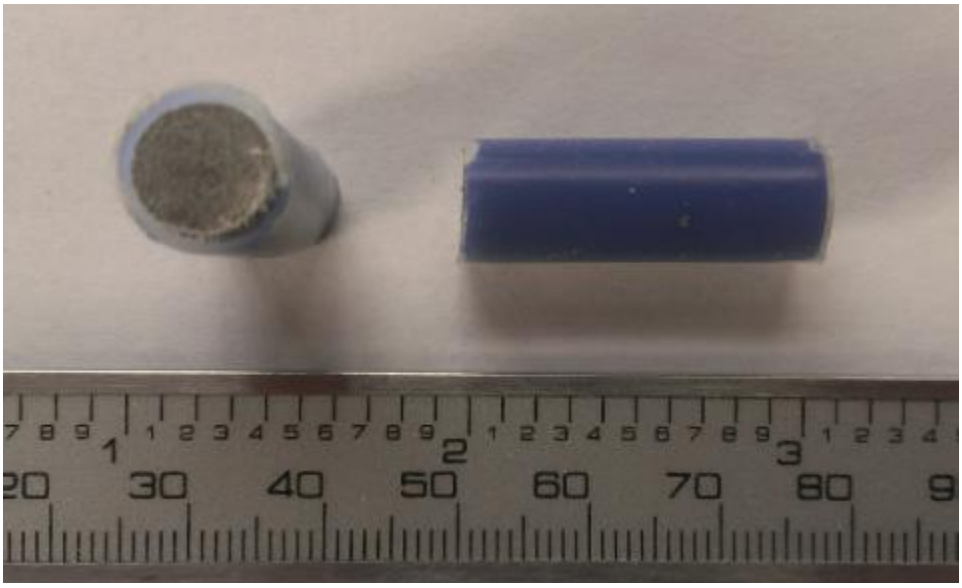

Figure 3: End-Product 1% Iron Additive Strands

3.3 Experimental Setup and Procedure

To measure the regression rate of solid propellants at elevated pressures, a new high-pressure strand burner experimental setup was created at RPI's Combustion and Energy Systems Laboratory. The experimental design, specifically ignition and pressure

monitoring were based off of similar designs in past literature (Carro, 2001). The centerpiece of this setup is a stainless steel 304 pressure chamber pictured in Figure 4. The chamber allows a maximum pressure of 175 atm but it has only been tested to about 110 atm. A removable bulkhead on the top of the chamber allows quick access to a spherical cavity of diameter 15.7 cm within the chamber. Three optical ports distributed around the sides of the chamber allow viewing into the cavity.

Figure 4: Strand-Burner Experiment Setup

Prior to the start of a test, the pressure chamber cavity is evacuated and filled with argon to provide an inert atmosphere for propellant burn rate measurements. The argon tank has a purity of 99.999%. Chamber pressure is monitored using a Setra 280E pressure transducer. Connections between the pressure transducer, pressure chamber, gas tank, and vacuum are linked by three Swagelok needle valves. Inside the pressure chamber cavity sits a custom-designed strand holder used to secure a single strand and elevate it into the center of one of the windows of the pressure chamber. The strand holder is made from pieces of SS304 cut and welded together at the RPI Machine Shop. The propellant is ignited using a nichrome wire held across the strand by two alligator clips epoxied to the strand holder. A Fisher Scientific Variable Autotransformer supplies the desired voltage across the nichrome wire. A MotionPro X3 camera sits outside the pressure chamber with the strand centered in its view so that the entire flame regression along the strands length

is visible. The camera is operated using the Motion Studio 64 program. A schematic of the entire setup is displayed in Figure 5.

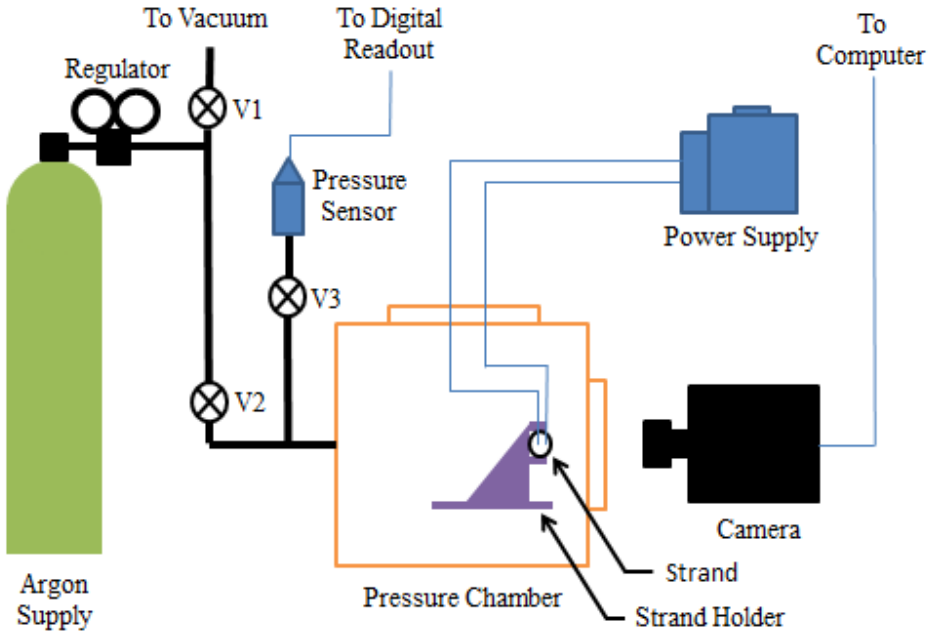

Figure 5: Strand-Burner Experiment Schematic

Prior to the start of a test, a single strand is massed on a Mettler AT200 electronic balance. The strand is then place in the strand holder in the horizontal direction and a nichrome wire is attached between the alligator clips so that it touches the igniting face of the propellant. The strand hold is then placed within the pressure chamber cavity and adjusted so that the strand is centered in the view of the camera and the entire axial length of the strand can be seen. The alligator clips are connected to the power supply via wire leads through the bulkhead of the pressure chamber. After bolting the bulkhead to the pressure chamber, the cavity is evacuated to 0.015 atm. Valve 1 is then closed and the strand burner is pressurized with argon to the desired ambient pressure. Chamber pressure is monitored using the Setra pressure transducer. After the desired pressure is reached, valves 2 and 3 are closed.

Once the setup is complete and the pressure chamber is sealed, the camera, set to record at 200 fps, is manually triggered. Immediately afterward, the power supply is switched on, provided ~10V across the nichrome wire to ignite the propellant.

Immediately after ignition, the power supply is switched off to avoid any sparking. The entire propellant strand is consumed within roughly 3 seconds, depending on propellant composition and chamber pressure. Figure 6 shows strand combustion at 50 atm as recorded by the MotionPro X3 camera. The flame front is clearly visible due to the high contrast settings and regresses into the propellant from right to left. An alligator clip used to hold the nichrome wire is visible at the right. After the test has concluded, the pressure chamber is pumped down to minimize the release of exhaust gases into the lab. After refilling the chamber with air, the bulkhead is removed and the chamber cavity is cleaned.

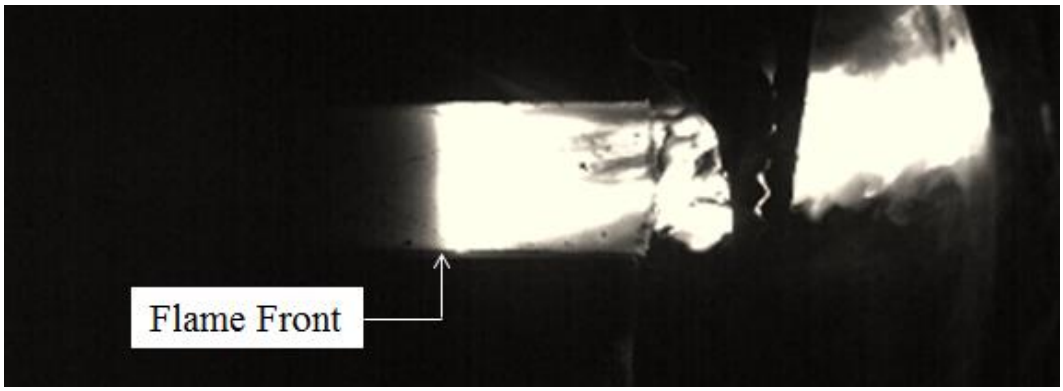

Figure 6: Camera Image of 1% Iron Strand Combustion at 50 atm

The recorded camera video from a single test is saved to a hard drive and the images are used to determine the burn rate. The start of flame regression is considered to be the ignition frame, or first appearance of flame on the igniting face, while the end of the test is the flame-out frame, the last frame where there's a flame is visible.

Since the recording frame rate is specified, the ignition and flame-out frames are known, and the strand length is known, the average regression rate can be calculated using Equation 3.

$$\dot{r} = \frac{L \times FR}{F_{fo} - F_{ign}} \tag{3}$$

For a single test the parameters of strand composition, strand mass, initial chamber pressure, and average regression rate are recorded.

3.4 Experimental Uncertainty

In order to minimize potential errors in the execution and measure of solid propellant combustion, many precautions have been taken and many redundancies have been added to the experimental process. Sources of error for the propellant composition are attributed to component massing and the mixing process. Sources of error for the regression rate calculation are the assumed strand length of 2.54 cm and the use of a camera frame numbers to determine burn time. Finally, the pressure transducer uncertainty and the addition of hot exhaust gases cause error in the ambient pressure measurement.

First, extreme care is taken when measuring propellant components to ensure that a batch's composition is as close as possible to the desired composition. The component masses are measured using a Mettler AT200 scale with precision to 0.0001g and any errors in composition are recorded. Errors in component mass are on the order of ±0.1% of the desired quantity. No density or composition non-uniformities have been noticed in any strands produced using the methods detailed in the mixing procedure section.

Similarly, caution is used when mixing the propellant to guarantee that all massed components are mixed without bits being left behind. The lengths of all strands are uniform due to the use of a jig and band saw for cutting the strands. The lengths of 5 strands were measured using a digital caliper with a precision of 0.001cm in order to confirm their uniformity. The samples had a mean length of 2.546 cm. Therefore, the assumption of a strand length of 2.54 cm introduces an estimated +0.2% error into the average regression rate calculation. Similarly, the use of ignition and flame-out frame numbers to determine burn time introduces error. Although the ignition and flame-out frames are easy to discern, the actual ignition or flame-out may occur between frames. For a frame rate of 200 fps and a typical burn time of ~3 seconds, a potential error by 1-2 frames implies a burn time error of ±0.33%. Although rare, any tests with uncertain ignition or flame-out frames are unused and were discarded. Cases in which the flame front propagates non-axisymmetrically were also discarded. The total uncertainty in the

average regression rate is estimated to be roughly ±0.5% (+0.53%, -0.13%). It should be noted that although the error on the regression rates of individual data points is relatively small, the actual regression rate between points may vary even for identical composition and chamber pressure. This variance is attributed to imperfections in composition measurement and anomalies or non-uniformities within individual strands.

Ambient chamber pressure is measured at the beginning of a test when the chamber is fully pressurized with argon. A Setra 280E pressure transducer is used to monitor the chamber pressure with an operable range of 0-204 atm and an accuracy of ±0.22 atm. The ambient chamber pressure recorded for each test is generally lower than the actual average pressure due to the addition of hot exhaust gases throughout the test. The actual ambient pressure in the chamber rises throughout a test, peaking at the time of flame-out. It was estimated using an ideal gas approximation that the consumption of a strand adds 0.94 atm of gas to the pressure chamber cavity. At low ambient pressures, this addition can be significant. Therefore, the total estimated pressure uncertainty is roughly +1 atm (+1.16 atm, +0.72 atm).

4. RESULTS AND DISCUSSION

Figure 7 shows the regression rate versus chamber pressure curve results for the baseline AP/HTPB composite solid propellant. The data is well-behaved and has relatively low scatter. The data is in excellent quantitative agreement with results found in the literature for AP/HTPB composite solid propellants with average AP particle sizes on the order of hundreds of microns and an AP to HTPB mass ratio of roughly 4:1 (Kohga, 2008 and Stephens, 2009). Figure 7 shows the comparison with the data produced by Kohga (2008). This also helps to validate the mixing method used and the experimental setup. The uncertainties associated with pressure and regression rate are shown on a single 10atm point. The actual chamber pressure is expected to be greater than the reported value due to the addition of exhaust gases during combustion. The uncertainty of the regression rate is almost negligible as the error bars barely show above the point. The values for temperature coefficient and pressure exponent are compiled in Table 2.

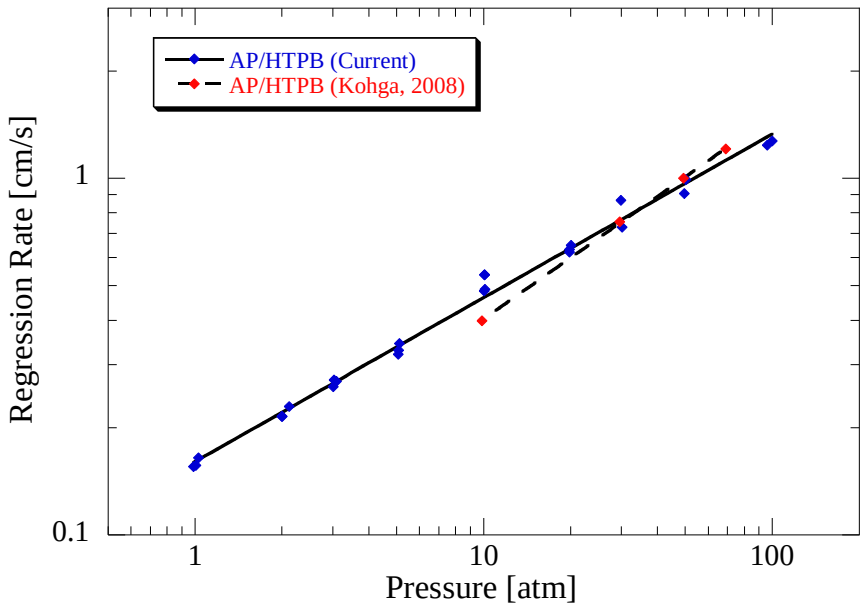

Figure 7: Regression Rate Versus Chamber Pressure for Baseline Solid Propellant

Figure 8 compares the regression rate versus chamber pressure data for AP/HTPB doped with 1% aluminum to that of the baseline propellant. Overall, the aluminum propellants show minimal scatter and excellent fit to the trend line. The results for both propellants are nearly identical, suggesting that a 1% addition of nano-aluminum has no effect on the baseline formulation. This result is interesting since aluminum is an additive that has been shown to increase the burn rate of AP-based solid propellants, at higher concentrations. Studies of aluminum additives to increase burn rate found in the literature studied propellants with aluminum composing roughly 15% of the strand's mass (Galfetti, 2007 and Jayaraman, 2009). However, the aluminum formulation used in this study is not necessarily comparable with literature mixtures. Regardless, it is interesting to note the lack of influence of the aluminum. Even an increase in thermal conductivity that would accompany the addition of metal could theoretically increase heat feedback into the propellant and therefore regression rate. However, Jayaraman et al. (2009) suggested that the burning rate for propellants with aluminum additives may decrease if the aluminum replaces coarse AP (as it does in this study) due to the reduction in the number of surface flamelets. Similarly, the accumulation of aluminum on the surface may act as a thermal sink, drawing heat away from the coarse AP grains. Therefore, it's suspected that there is a balance between increased heat feedback, the increased thermal sink away from AP particles, and decreased surface flamelets in AP composite solid propellants with small amounts of aluminum added. The values of the temperature coefficient and pressure exponent for the 1% aluminum trend line are given in Table 2.

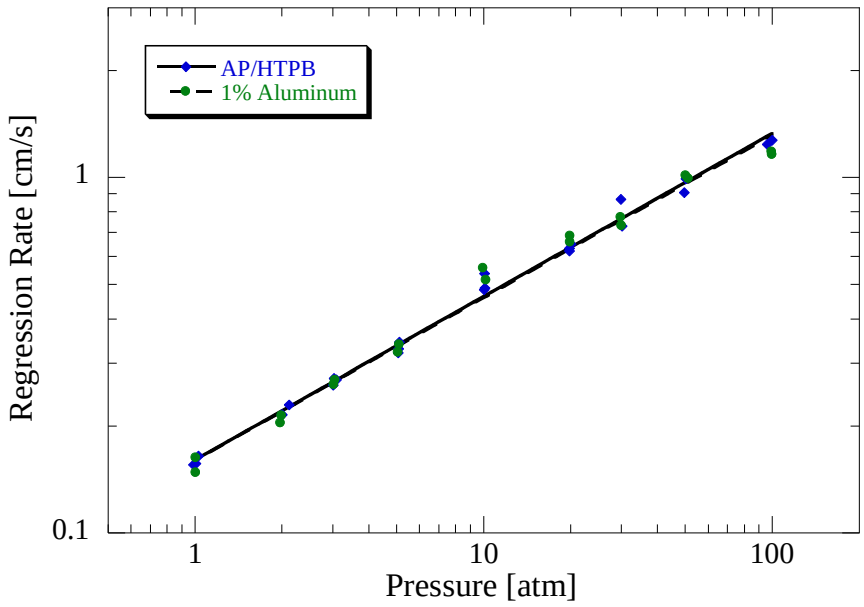

Figure 8: Regression Rate Versus Chamber Pressure for Baseline and 1% Aluminum Formulations

The addition of 1% iron to the baseline AP/HTPB formulation produces a significant increase in burn rate for all pressures. Figure 9 shows that the burn rate increase above the baseline is lower at 1 atm and at high pressures. The 1% iron curve appears to show consistent reduced burning rate behavior above 30 atmospheres. The exact reason for this is uncertain, but it may be due to a change in the flame structure above the coarse AP particles at higher pressures, as suggested by the BDP model. The iron tests also show a greater degree of scatter compared to the aluminum tests. Regardless, the increase in burn rate is measurable and significant (~2x). This result is somewhat surprising, considering the null result found in the 1% aluminum study. In general, iron has a lower thermal conductivity and a lower melting temperature than aluminum, suggesting that there is less heat feedback and less heat sink in the iron propellants. The results seem to suggest that iron may even act as a chemical catalyst in AP decomposition or gas-phase reactions. The reduced burn rate at high pressures, when the diffusion flame becomes secondary to the AP monopropellant flame, suggests that iron is more likely to act as a catalyst to the gas-phase reactions. None of the literature

found contained experiments on nano-scale iron additives. The values for temperature coefficient and pressure exponent for the 1% iron trend line are given in Table 2.

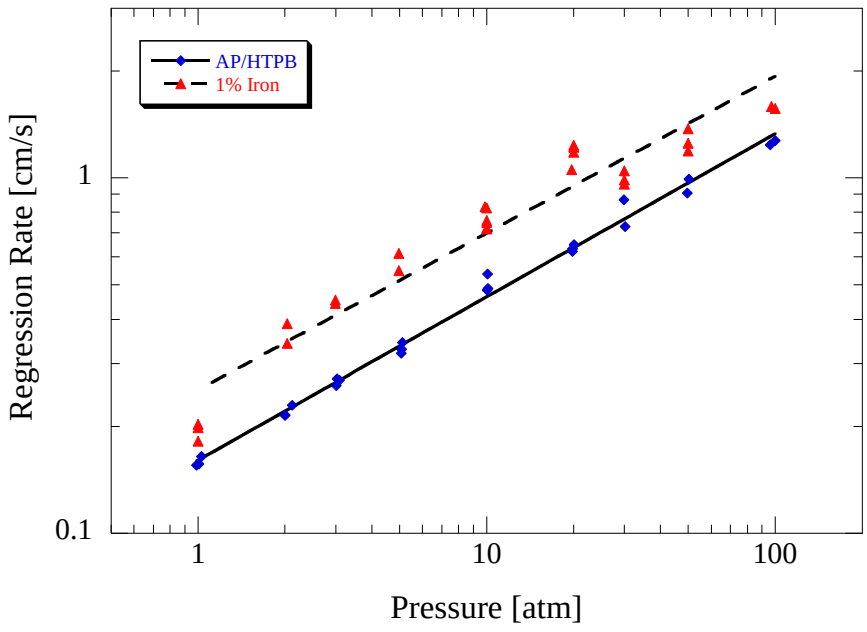

Figure 9: Regression Rate Versus Chamber Pressure for Baseline and 1% Iron Formulations

Table 2 shows the temperature coefficients and pressure exponents associated with the baseline, 1% aluminum, and 1% iron curves. The baseline and 1% aluminum constants are nearly identical while the 1% iron curve has a higher temperature coefficient but nearly identical pressure exponent. The constants are found for an equation in the form of Equation 1 with pressure units of atm and regression rate units of cm/s.

Table 2: Temperature Coefficients and Pressure Exponents for Baseline, 1% Aluminum, and 1% Iron Formulations of the Current Study

Formulation	Temperature Coefficient (a)	Pressure Exponent (n)
Baseline	0.1605	0.4597
1% Aluminum	0.1602	0.4576
1% Iron	0.2531	0.4413

Since the addition of iron was shown to have a positive effect on the baseline propellant, the amount of iron added to the composite solid propellant was theorized to have an effect as well. Figure 10 shows the regression rate of the solid propellant as a function of iron concentration. The red data points depict the mean values of multiple tests conducted at each concentration. The error bars associated with the mean values are the standard deviations of the regression rates of the tests at each additive percentage. The data contains some scatter at all concentrations. However, the scatter is about the same as the scatter shown in the regression rate vs. pressure curve for 1% iron. Originally, only concentrations of 0.5, 1, 2, and 3% were to be tested. However, the nonlinear drop in mean regression rate from 1 to 2% warranted extra tests to increase resolution. The mean regression rate values at 1.25 and 1.5% confirmed the drop in regression rate from 1 to 2%. The physical reason for this trough is uncertain, but it may be linked to additional iron accumulation and heat sink away from AP flamelets. The regression rate has a local maximum at 1%. At 3% iron, the propellant achieved the highest mean regression rate, possibly due to the ignition of iron accumulated at the surface. This phenomenon was proposed by Jayaraman et al. (2009) for aluminum and increased burn rate. Regardless of the percentage of iron added, the regression rate is still higher than that of baseline AP/HTPB. The percentage increases in average regression rate above the baseline formulation is given in Table 3. Tests were performed with 5% iron additive but the combustion of the strand created a thick black smoke that often obscured the flame out frame, leading to an uncertain burn rate. Therefore, the 5% iron additive tests are unused. The error bars associated with regression rate and additive percentage are shown on a single point at 1.5% additive. Both uncertainties are very small.

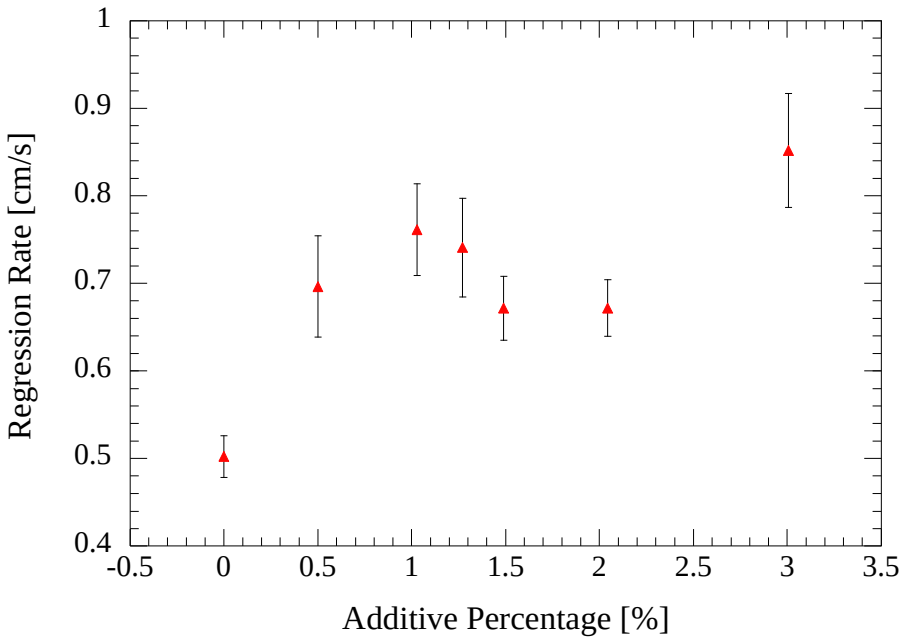

Figure 10: Regression Rate Versus Iron Additive Percentage at 10 atm for Iron Additive Formulations

Table 3: Percent Increase in Mean Regression Rate Compared to the Baseline Formulation

Iron Concentration [%]	Mean Regression Rate Increase
0.5	38.64
1	51.58
1.25	47.52
1.5	33.7
2	33.78
3	69.59

5. FUTURE WORK

Although the literature review required by this project was relatively extensive, multiple sources reviewed contained detailed literature reviews as well. Due to this, and the long history of solid propellant tailoring, there is still a plethora of information that has yet to be examined in detail. We suggest that the literature review section provided here be expanded, specifically with sources cited by Cai, Thakre, and Young (2008), Stephens et al. (2009), and Jayaraman et al. (2009).

Since the results presented here are the first solid propellant results out of the new RPI strand burner experiment, the research group expects numerous studies regarding solid propellant additives to be produced in the future. Before new tests proceed, however, it's desired that the strand burner setup itself is further validated with propellants and additives that have already been catalogued in literature. This study found that the mechanism by which iron enhances the burn rate of AP/HTPB solid propellants is uncertain. Solid propellant modeling or flame temperature data for a range of pressures and additive concentrations would be useful in determining this mechanism. New experiments on the effects of catalytic additives in combination with metal additives should be performed as well. Finally, the research group plans to add studies on the effects of carbonaceous additives, such as graphene and CNTs, in the future.

LITERATURE CITED

Kohga, M. (2008). Burning rate characteristics of ammonium perchlorate-based composite propellant using bimodal ammonium perchlorate. *Journal of Propulsion and Power, 24*(3), 499-506.

Summerfield, M., Steinz, J. A., & Stang, P. L. (1969). *The burning mechanism of ammonium perchlorate-based composite solid propellants* (Aerospace and Mechanical Sciences Report No. 830). Princeton, NJ: Princeton University, Department of Aerospace and Mechanical Sciences.

Stephens, M. A., Petersen, E. L., Reid, D. L., Carro, R., & Seal, S. (2009). Nano additives and plateau burning rates of ammonium-perchlorate-based composite solid propellants. *Journal of Propulsion and Power, 25*(5), 1068-1078.

Stone, M. W. (1958). A practical mathematical approach to grain design. *Journal of Jet Propulsion, 28*(4), 236-244.

Parr, T., & Hanson-Parr, D. (1996). Solid propellant diffusion flame structure. *Proceedings of the Combustion Institute, 26*(2), 1981-1987.

Sutton, G. P., & Biblarz, O. (2010). *Rocket propulsion elements* (8th ed.). Hoboken, NJ: John Wiley & Sons, Inc.

Fujimura, K., & Miyake, A. (2010). The effect of specific surface area of TiO2 on the thermal decomposition of ammonium perchlorate. *Journal of Thermal Analysis and Calorimetry, 99*(1), 27-31.

Chen, X., & Mao, S. S. (2006). Synthesis of titanium dioxide (TiO_2) nanomaterials. *Journal of Nanoscience and Nanotechnology, 6*(4), 906-925.

Hermance, C. E. (1966). A model of composite propellant combustion including surface heterogeneity and heat generation. *AIAA Journal, 4*(9), 1629-1637.

Beckstead, M. W., Derr, R. L., & Price, C. F. (1970). A model of composite solid-propellant combustion based on multiple Flames. *AIAA Journal, 8*(12), 2200-2207.

Glick, R. L. (1974). On statistical analysis of composite solid propellant combustion. *AIAA Journal, 12*(3), 384-385.

Renie, J. P. (1982). *Combustion modeling of composite solid propellants* (Doctoral dissertation). Retrieved from Purdue University AAE Library Theses and Dissertations Database.

King, M. K. (1978, January). *Model for steady state combustion of unimodal composite solid propellants*. Paper presented at the AIAA 16th Aerospace Sciences Meeting, Huntsville, AL.

King, M. K. (1981). Experimental and theoretical study of the effects of pressure and crossflow velocity on composite propellant burning rate. *Proceedings of the Combustion Institute, 18*(1), 207-216.

Cor, J. J. (1986). *A continuous oxidizer regression model for the combustion of composite solid propellants* (Master's thesis). Retrieved from DTIC Online. (ADA186742)

Hegab, A., Jackson, T., Buckmaster, J., & Stewart, D. (2001). Nonsteady burning of periodic sandwich propellants with complete coupling between the solid and gas phases. *Combustion and Flame, 125*(1-2), 1055-1070.

Massa, L., Buckmaster, J., & Jackson, T. L. (2005). New kinetics for a model of heterogeneous propellant combustion. *Journal of Propulsion and Power, 21*(5), 914-924.

Ramakrishna, P., Paul, P., & Mukunda, H. (2002). Sandwich propellant combustion: Modeling and experimental comparison. *Proceedings of the Combustion Institute, 29*(2), 2963-2973.

Cai, W., Thakre, P., & Yang, V. (2008). A model of AP/HTPB composite propellant combustion in rocket-motor environments. *Combustion Science and Technology, 180*(12), 2143-2169.

Gross, M. L., & Beckstead, M. W. (2011). Steady-state combustion mechanisms of ammonium perchlorate composite propellants. *Journal of Propulsion and Power, 27*(5), 1064-1078.

Gross, M. L., & Beckstead, M. W. (2009). Diffusion flame calculations for composite propellants using a vorticity-velocity formulation. *Journal of Propulsion and Power, 25*(1), 74-82.

Collins, H. L. H. (1947). *Experimental study of the burning rates of some solid propellants by using a closed bomb* (Professional thesis). Retrieved from Caltech THESIS Database.

Renie, J. P., Condon, J. A., & Osborn, J. R. (1979). Oxidizer size distribution effects on propellant combustion. *AIAA Journal, 17*(8), 877-883.

Cohen, N. S., Derr, R. L., & Fleming, R. W. (1974). Role of binders in solid propellant combustion. *AIAA Journal, 12*(2), 212-218.

Jayaraman, K., Anand, K., Chakravarthy, S., & Sarathi, R. (2009). Effect of nano-aluminium in plateau-burning and catalyzed composite solid propellant combustion. *Combustion and Flame, 156*(8), 1662-1673.

Pearson, G. S. (1971). The role of catalysts in the ignition and combustion of solid propellants. *Combustion Science and Technology, 3*(4), 155-163.

Solymosi, F., Gera, L., & Börcsök, S. (1971). Catalytic pyrolysis of $HClO_4$ and its relation to the decomposition and combustion of NH_4ClO_4. *Proceedings of the Combustion Institute, 13*(1), 1009-1017.

Rastogi, R., Singh, G., & Singh, R. R. (1977). Burning rate catalysts for composite solid propellants. *Combustion and Flame, 30*, 117-124.

Strahle, W. C., Handley, J. C., & Milkie, T. T. (1974). Catalytic effects in the combustion of AP-HTPB sandwiches to 3200 PSIA. *Combustion Science and Technology, 8*(5-6), 297-304.

Handley, J. C., & Strahle, W. C. (1975). Behavior of several catalysts in the combustion of solid propellant sandwiches. *AIAA Journal, 13*(1), 5-6.

Chakravarthy, S. R., Price, E. W., & Sigman, R. K. (1997). Mechanism of burning rate enhancement of composite solid propellants by Ferric Oxide. *Journal of Propulsion and Power, 13*(4), 471-480.

Stephens, M., Petersen, E., Carro, R., Reid, D., & Seal, S. (2010). Multi-parameter study of nanoscale TiO_2 and CeO_2 additives in composite AP/HTPB solid propellants. *Propellants, Explosives, Pyrotechnics, 35*(2), 143-152.

Kreitz, K. R. (2010). *Catalytic nanoparticle additives in the combustion of AP/HTPB composite solid propellant* (Master's thesis). Retrieved from Texas A&M University Libraries Database.

Yaman, H., Çelik, V., & Değirmenci, E. (2014). Experimental investigation of the factors affecting the burning rate of solid rocket propellants. *Fuel, 115*, 794-803.

Galfetti, L., Deluca, L., Severini, F., Colombo, G., Meda, L., & Marra, G. (2007). Pre and post-burning analysis of nano-aluminized solid rocket propellants. *Aerospace Science and Technology, 11*(1), 26-32.

Sambamurthi, J. K., Price, E. W., & Sigman, R. K. (1984). Aluminum agglomeration in solid-propellant combustion. *AIAA Journal, 22*(8), 1132-1138.

Liu, L., Li, F., Tan, L., Ming, L., & Yi, Y. (2004). Effects of nanometer Ni, Cu, Al and NiCu powders on the thermal decomposition of ammonium perchlorate. *Propellants, Explosives, Pyrotechnics, 29*(1), 34-38.

Carro, R. V. (2001). *High pressure testing of composite solid rocket propellant mixtures: Burner facility characterization* (Master's thesis). University of Central Florida Electronic Theses and Dissertations Database. (CFE0001979)